Colloidal particles at a nematic-isotropic interface: effects of confinement

John L. West and Ke Zhang
Liquid Crystal Institute, Kent State University, Kent, Ohio 44242, USA

Anatoliy Glushchenko
University of Colorado at Colorado Springs, Colorado Springs, CO 80933, USA

Denis Andrienko
Max-Plank Institute for Polymer Research, Ackermannweg 10, Mainz 55128, Germany and
Liquid Crystal Institute, Kent State University, Kent, Ohio 44242, USA

Mykola Tasinkevych
Max-Planck-Institut für Metallforschung, Heisenbergstr. 3, Stuttgart 70569, Germany and
Institut für Theoretische und Angewandte Physik,
Universität Stuttgart, Pfaffenwaldring 57, Stuttgart 70569, Germany

Yuri Reznikov
Institute of Physics, Prospect Nauky 46, Kyiv 03039, Ukraine
(Dated: February 6, 2008)

When captured by a flat nematic-isotropic interface, colloidal particles can be dragged by it. As a result spatially periodic structures may appear, with the period depending on a particle mass, size, and interface velocity [1]. If liquid crystal is sandwiched between two substrates, the interface takes a wedge-like shape, accommodating the interface-substrate contact angle and minimizing the director distortions on its nematic side. Correspondingly, particles move along complex trajectories: they are first captured by the interface and then 'glide' towards its vertex point. Our experiments quantify this scenario, and numerical minimization of the Landau-de Gennes free energy allow for a qualitative description of the interfacial structure and the drag force.

I. INTRODUCTION

Precise manipulation of tiny particles in liquids is a rapidly developing direction of a modern technology. Manufacturing of *e*-papers and electrophoretic displays [2, 3], separation of bacterial species and living cells [4, 5, 6], trapping of DNA and polymer particles [7, 8, 9], growth of photonic crystals [10, 11], are only a few examples revealing its scientific and technological importance.

In order to move, organize, or separate colloidal particles several techniques have been suggested, among them the drag of the micro-particles by a moving nematic-isotropic interface [1]. Briefly, due to the interfacial and surface tensions as well as long-range distortions of the director field, particles can be captured and subsequently dragged by the moving interface. Matching the speed of the interface, particle size, and elastic properties of the liquid crystal, one can move particles of specified radius and control their spatial distribution in the cell.

In our previous work [1] we consider the situation when the interface between the nematic and isotropic phases is flat. In a slab geometry, however, the interface bends accommodating the contact angle between the nematic phase, the isotropic phase, and the substrates, and minimizing the director distortions on the nematic side of the interface [12, 13]. As a result, the meniscus of the isotropic phase extends into the nematic phase; this of course influences particle trajectories in the interfacial
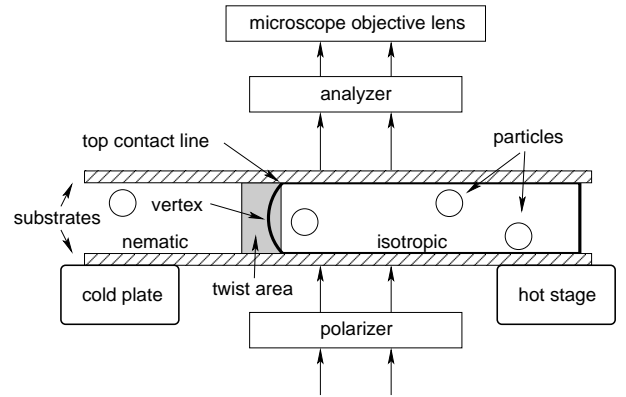

FIG. 1: Experimental setup.

region. In this paper we study the behavior of colloidal particles captured by a wedge-shaped interface. We first examine the shape of the interface and the director distribution in its vicinity. Then we analyze how these factors influence the trajectory of a particle in the interfacial region. We conclude that there is an additional force on a particle acting towards the vertex of the interface. Finally, we compare our experimental results to the estimates based on the minimization of the Landau-de Gennes free energy.
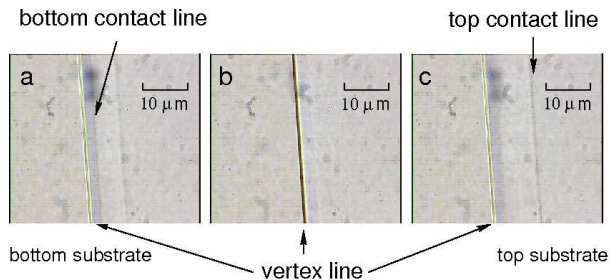
FIG. 2: Typical optical images of the extended interface. The microscope objective lens is focused on a) bottom substrate; b) vertex line, cell bulk; c) top substrate.

FIG. 3: Snapshot of the moving interface. Hot stage cooling speed 5deg/min. Orientations of the polarizer (P) and analyzer (A) are marked by the white arrows. Rubbing direction is parallel to the horizontal side of the pictures.

II. EXPERIMENT

Spherical polystyrene particles of diameter $d = 16\,\mu$m are dispersed in the isotropic phase of liquid crystal 5CB using ultrasonic shaker. The density of the particles, $1.04\,$g/cm^3, is slightly higher than the density of pure 5CB, $1.007\,$g/cm^3 [14]. The surface of the particles provides planar alignment of the liquid crystal director. $40\,\mu$m-thick cells are filled with the mixture in the isotropic phase and cooled to room temperature. The uniform planar alignment is obtained by rubbing layers of polyamide PI2555 deposited on the substrates.

The experimental setup is sketched in Fig. 1 and is described in detail in Ref. [1]. Briefly, one end of the cell is placed on a hot stage; the other end is attached to a metal plate, kept at a room temperature. The temperature of the hot plate could be changed with the speed 0.1 deg/min and is monitored with the accuracy 0.05 deg. Typical temperature gradients over the cell are $20-30\,$deg/cm. Heating/cooling of the hot stage with the speed 5 deg/min results in the interface movement with the speed $v \approx 13\,\mu$m/s. The system is observed through the polarizing microscope.

Typical optical images of the cell are shown in Fig. 2. Two homogeneous phases are separated by a rather wide, birefringent, region. The width of this region depends on the speed of the interface. In a stationary case it is about $10\,\mu$m, which corresponds to $0.025^0\,$C; at $13\,\mu$m/s it is about $40\,\mu$m. The region occupied by the extended interface has a distinct boundary which separates it from the nematic side of the cell. We denote this boundary as a vertex line. Focusing the microscope lens on the cell substrates, we observed two additional lines positioned on the right side of the vertex line, in the isotropic phase, see Figs. 2(a) and (c), contact lines. The vertex line is also visible here, however it is less sharp compared to the situation when the focus is on the bulk of the cell, Fig. 2(b).

These observations allow us to reconstruct the shape of the interface. Since the nematic phase of 5CB wets polyamide-treated surfaces [15, 16], the interface bends
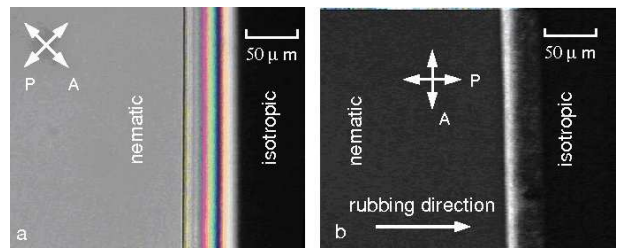
in order to accommodate the zero contact angle at the cell substrates [12, 16, 17]. This bending influences the director distribution in the cell. The director is anchored at the interface with the tilt angle $\theta \approx 26.5\,$deg and rather strong anchoring, $W \approx 10^{-3}\,$erg/cm^2 [18]. The substrates provide planar orientation of the director. To match the boundary conditions at the interface and the substrates, the director orientation must change from the uniform planar orientation far from the interface to the tilted orientation at the interface.

Rotating the cell between crossed polarizers we have also noticed that the director is parallel to the rubbing direction everywhere except close to the vertex line, see Fig.3(a). This region looked bright between crossed polarizers on the background of the remaining, dark cell, see Fig.3(b). Rotating the analyzer we were able to darken the region next to the vertex line. From these observations we concluded that, close to the vertex line, the the director twists in the xz plane, parallel to the substrates. The value of the twist angle was not well reproducible, changing from 45 to 90 degrees.

Director twist can be understood qualitatively, in terms of the splay-bend and twist contributions to the elastic energy. Next to the vertex line the director has significant splay-bend deformation, which is energetically unfavorable. It is known that the director can relax this deformation by twisting in the perpendicular plane [19, 20, 21, 22]. The balance of the elastic energies of the twist and splay-bend deformations defines if twist occurs or not. Since the twist elastic constant K_{22} for 5CB is about two times smaller than the splay and bend elastic constants, K_{11} and K_{33}, it is energetically more favorable for the director to twist than to bend. In fact, such an 'escape' of the director has already been observed in a similar system, where the nematic is in the contact with its own melt [12] or with air [13].

Now that the shape of the interface and the director distribution in the interfacial region are known, let us have a look at the motion of colloidal particles. Upon cooling of the hot stage, the area occupied by the nematic phase grows; the interface moves towards the hot stage, meeting the particles dispersed in the isotropic
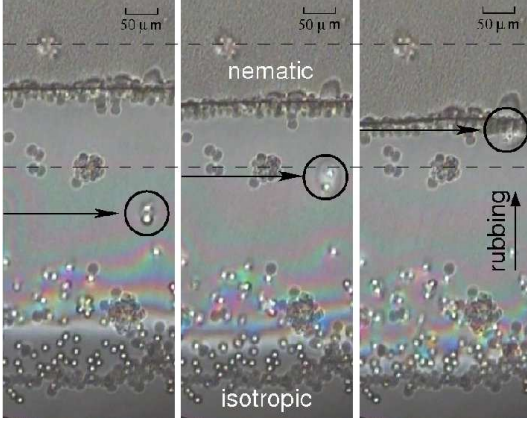
FIG. 4: Snapshots of a moving nematic-isotropic interface, separated by the 2s time intervals, which illustrate particle attraction to the vertex line before it is captured by the interface. Two dotted lines show the position of two aggregates which are stuck to the cell surface and serve as reference points. The interface moves slowly from the top to the bottom; at the same time, a cluster of two colloidal particles (encircled by a solid line) moves towards the interface, from the bottom to the top.

FIG. 5: Schematic representation of the capillary force $\mathbf{F}_c$ and the drag force $\mathbf{F}_d$ exerted on a colloidal particle by the moving nematic-isotropic interface. Projection $\mathbf{F}_u$ of the capillary force onto the y axis (perpendicular to the substrates) pushes the particle towards the vertex point.

FIG. 6: Snapshots of the moving interface. The three particles are attracted to the interface and, because of the vertical motion, disappear from the focus (near the NI line, snapshots 4 and 5). In order to see them in the focus again, we need to change the focal distance from $z = 90\mu m$ to $z = 60\mu m$ (snapshot 6), where z is a vertical distance from the objective lens to some arbitrary level. Experiments were made with $16\mu m$ particles in a $200\mu m$ thick cell.

phase. Fast moving interfaces with the velocity above $18\,\mu$m/s are not able to capture the particles. At smaller velocities, dispersed in the isotropic phase particles are attracted to the interface as soon as they reach one of the contact lines, as illustrated in Fig. 4. Immediately after that they speed up towards the vertex line, in the direction opposite to the interface propagation. Upon reaching the vertex line, particles reverse the direction of motion and start following the interface. In fact, even when the particles are deep in the isotropic phase, there is a small force acting on them in the direction opposite to the temperature gradient, i.e., towards the interface. This force is due to increase of the free energy of a paranematic phase at the surface of the particle when it moves into the region with a higher temperature.

Upon heating, the interface moves away from the hot stage, pushing the particles from the isotropic to the nematic phase. Particles start to interact with the interface only at a distance comparable to their own diameter and much smaller speeds of the interface, below $4\,\mu$m/s, are required to capture them.

To understand particle dynamics we first note that the density of the particles is slightly bigger than the density of the liquid crystal. As a result, they gradually sediment at the bottom substrate, where they meet the moving interface. If a particle is trapped by the interface, the interfacial tension results in a force on the particle, directed perpendicular to the interface.

Since the particle is moving with the interface it experiences Stokes drag force in the direction opposite to the velocity of the interface. If the velocity of the par-
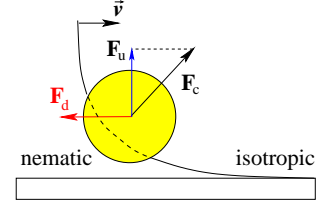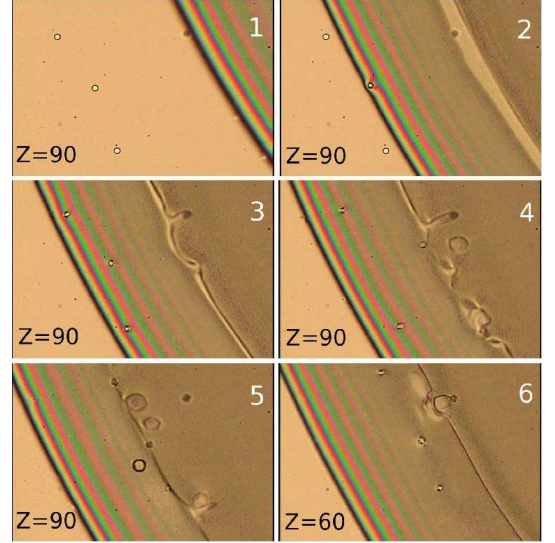
ticle does not change, then the sum of all forces on the particle is zero. This means that the elastic plus capillary forces shall compensate the drag force. However, the latter has only the x-component, in the direction of the interface velocity. At the same time, the capillary force is perpendicular to the interface and has a component pointing towards the vertex point, as shown in Fig. 5. Hence, the particle will move until this component of the force vanishes, which is at the vertex point.

In addition, in order to minimize the elastic free energy of the system, the particle tries to occupy the place with the strongest distortions of the director [23]. This results in an additional force guiding the particle towards
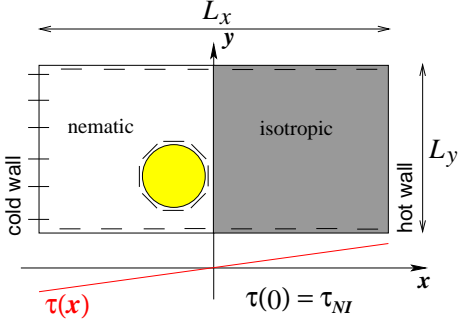
FIG. 7: Sketch of the xy cross-section of the system. System size $L_x \times L_y$. Boundary conditions: planar alignment of the nematic director at the particle and cell surfaces. Initial conditions: flat nematic-isotropic interface at $x = 0$.

the vertex line. Together, these two forces lift the particle in the cell, in the direction opposite to the interface propagation. In fact, the particle lifting can be directly observed by changing the focal distance of the objective lens, as shown in Fig. 6.

To support these arguments, in the following we study the behavior of the colloid in the vicinity of the confined nematic-isotropic (NI) interface in the framework of Landau-de Gennes free energy.

III. THEORETICAL MODEL AND DISCUSSION

A geometry mimicking the experimental setup is shown in Fig. 7. A uniform temperature gradient is imposed along the x axis with the 'hot' wall at $x = L_x/2$ and the 'cold' wall at $x = -L_x/2$. The director at the 'cold', bottom and top walls is fixed in the x-direction, and the absolute value of the order parameter at these walls is fixed to the bulk order parameter of the nematic phase at two-phase coexistence. The order parameter at the 'hot' wall is set to zero. A colloidal particle, which we take to be a long cylinder of radius R, with the symmetry axis parallel to the z axis, imposes rigid planar anchoring boundary conditions at its surface. This results in the formation close to the colloid of two topological defects, known as boojums [24]. The defects are aligned in the direction of the liquid crystal alignment, i.e., parallel to the x axes.

The system is described by the Landau-de Gennes free energy [25]

$$\mathcal{F}\{\boldsymbol{Q}\} = \int (f_b + f_e) dV \qquad (1)$$

where f_b is the bulk free energy density and f_e is the elastic free energy density. The minimum of the Landau-de Gennes functional $F\{\boldsymbol{Q}\}$ gives the equilibrium value of the tensor order parameter $\boldsymbol{Q}$. Symmetry arguments yield the bulk free energy density [25, 26]

$$f_b = a(T - T^*)\mathrm{Tr}\boldsymbol{Q}^2 - b\mathrm{Tr}\boldsymbol{Q}^3 + c\left[\mathrm{Tr}\boldsymbol{Q}^2\right]^2, \qquad (2)$$

where the positive constants a, b, c are taken temperature independent. It is convenient to scale out the variables by defining

$$\tilde{Q}_{ij} = 6c/bQ_{ij}, \qquad (3)$$
$$\tilde{f}_b = 24^2 c^3/b^4 f_b.$$

It will be understood that such scaling has been carried out, and we shall omit the over-bars in the text below. We also introduce a dimensionless temperature τ by defining

$$a(T - T^*) = \tau b^2/24c. \qquad (4)$$

The bulk nematic phase is stable for $\tau < \tau_{\mathrm{NI}} = 1$ with a degree of orientational order given by $Q_b = 3(1 + \sqrt{1 - 8\tau/9})/4$; $Q_b(\tau > 1) = 0$. We model the temperature gradient in the x direction by assuming that τ changes linearly with the x coordinate

$$\tau = \tau_{NI}(1 + \alpha x). \qquad (5)$$

Equation (5) implies that the NI transition occurs at $x = 0$, and that the unconfined interface would form in the yz plane.

We assume strong planar (parallel) anchoring of the director with the particle surface. This is valid if the anchoring parameter $WR/K >> 1$, where W is the anchoring energy of the particle surface, and holds for relatively large colloidal particles or big anchoring strengths. We also assume that the nematic phase at the particle surface is uniaxial with a scalar order parameter $Q_s = 1$.

The elastic free energy density can be written as [26]

$$f_e = \frac{1}{2}L_1 \frac{\partial Q_{ij}}{\partial x_k}\frac{\partial Q_{ij}}{\partial x_k} + \frac{1}{2}L_2 \frac{\partial Q_{ij}}{\partial x_j}\frac{\partial Q_{ik}}{\partial x_k}, \qquad (6)$$

where the constants L_1 and L_2 are related to Frank-Oseen elastic constants by $K_{11} = K_{33} = 9Q_b^2(L_1 + L_2/2)/2$ and $K_{22} = 9Q_b^2 L_1/2$ and Q_b is the bulk nematic order parameter.

We use typical values of the material parameters available for 5CB [32, 33]: $a = 0.044 \times 10^6 \mathrm{J/m^3K}$, $b = 0.816 \times 10^6 \mathrm{J/m^3}$, $c = 0.45 \times 10^6 \mathrm{J/m^3}$, $L_1 = 6 \times 10^{-12}\mathrm{J/m}$, $L_2 = 2L_1$, $T^* = 307\mathrm{K}$. The nematic-isotropic transition temperature for 5CB is $T_{NI} = 308.5\,\mathrm{K}$.

A. Shape of the interface

We minimize the free energy (1) numerically, using finite elements with adaptive meshes. The area $L_x \times L_y$ is triangulated and the order tensor $\boldsymbol{Q}$ is set at all vertices of the mesh and is linearly interpolated within each triangle [27, 28, 29]. The free energy is then minimized using conjugate gradients method under the constraints imposed by the boundary conditions.

In the experiment, the $40\,\mu\mathrm{m}$ cells are filled with the $16\,\mu\mathrm{m}$ colloidal particles. To minimize computational efforts, we reduce the system size to $L_y = 3\,\mu\mathrm{m}$. In fact,
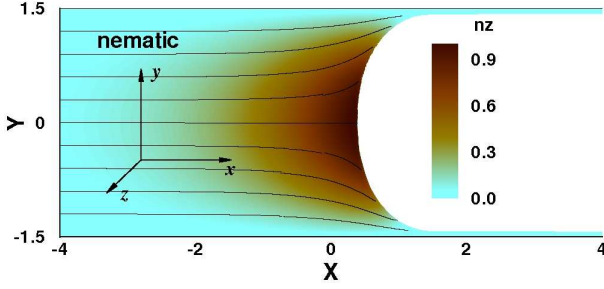
FIG. 8: Cross-section of the cell with the nematic-isotropic interface. Color coding shows the n_z, out of plane, component of the director. The director is practically parallel to the z axis close to the interface (twist angle $\approx \pi/2$, $n_z \approx 1$). $L_x = 15\mu m$, $L_y = 3\mu m$. The temperature gradient parameter $\alpha = 0.0036\mu m^{-1}$, which corresponds to $\approx 54 deg/cm$.

minimization of the free energy in a system of this size is a nontrivial task: the smallest length scale involved in the problem is given by the thickness of the interface, which is of the order of the nematic coherence length at coexistence, $\xi = (24L_1 c/b^2)^{1/2} \approx 10\,\text{nm}$. This length scale sets the mesh size. Thus, about 10^7 mesh points would be required for a rectangular uniform discretization of the cell. By using adaptive meshes we are able to reduce this number by more than two orders of magnitude, which makes the minimization procedure computationally feasible.

We first have a look at the shape of the interface without colloidal particle. The chosen anisotropy of the elastic constants, $L_2/L_1 = 2$, favors director alignment parallel to the NI interface, which is in mismatch with the boundary conditions at the cell boundaries. As we have already mentioned in the previous section, this leads to formation of the curved interface. The contour plot of the n_z (out of plane) component of the director and the stream-traces of the in-plane (n_x and n_y) components are shown in Fig. 8. The interface is quasi-flat in the middle of the cell and curved at the horizontal surfaces of the box. To avoid strong in-plane splay-bend deformations, the director twists at the interface, in a qualitative agreement with the experimental results. The twist angle at the interface reaches $\pi/2$, i. e. the director is parallel to the interface and the substrates. Experimentally observed twist angle is smaller, of the order of $\pi/4$. The difference between the experimentally measured and calculated values is due to the different anchoring of the director at the interface: for 5CB this angle is about 26 deg, whereas our model (which takes into account only second-order terms in the gradient expansion) predicts planar interfacial anchoring. The shape of the interface is symmetric, with its vertex point placed in the middle between the walls, which is in disagreement with the experiment, where slightly asymmetric interfacial profile is observed. The asymmetry of the experimental interfaces is most probably due to the non-zero temperature
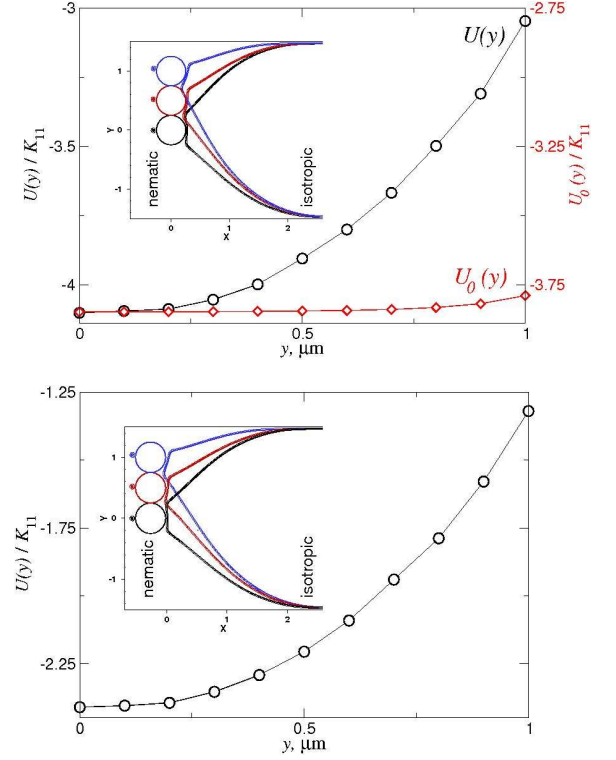

FIG. 9: Free energy $U(y)$ per unit length (circles). Colloid radius $R = 0.25\,\mu m$, system size $9 \times 3\,\mu m$. Temperature gradient $\alpha = 0.001\mu m^{-1}$ which corresponds to $\approx 15 deg/cm$. Insets illustrate the shape of the interface for different positions of the colloidal particle. Upper panel: $x = 0$; lower panel $x = -0.27\mu m$. $U_0(y)$ (shown in the upper panel, diamonds) is the free energy of a colloidal particle in a pure nematic phase, at $\tau = \tau_{NI}$. $K_{11} \approx 4.93 \times 10^{-12}$ J/m for $\tau = \tau_{NI} = 1$.

gradient across the cell (along the y axis).

B. Forces on a particle in the interfacial region

Now let us focus on the interaction of a colloidal particle with the NI interface. In our previous work [1, 29] we have shown that a single colloidal particle is attracted by a *flat* interface, with the force which is roughly proportional to the particle radius. This force drags the particles along the direction of the temperature gradient (x-axis). However, because of the wedge-like shape of the interface, one can also expect an additional component of the force, along the y axis. To calculate this component, we placed a test particle, modeled as a long cylinder of radius $R = 0.25\,\mu m$ with the symmetry axis parallel to the z axis, next to the interface and evaluated the free energy of the system as a function of the y-position of the particle, at the fixed x-position. To improve the computational efficiency, the system size was further decreased to $9 \times 3\,\mu m$.

The free energy $U(x = const, y) \equiv U(y)$ per length

of the colloidal particle is shown in the Fig. 9 for two values of the x-position of the colloid. The temperature gradient parameter $\alpha = 0.001\mu m^{-1}$, corresponding to $\approx 15 deg/cm$. In both cases $U(y)$ has a minimum when the particle is in the middle of the cell, at $y = 0$. At any other point there is a non-zero force $F_y = -\partial \mathcal{F}/\partial y$, which pulls the particle towards the middle of the cell (upwards, if it is placed at the bottom wall). Therefore, even when the interface is not moving, those particles which are captured by the interface tend to cluster in the middle of the cell, at the vertex line.

Because of the fixed anchoring conditions imposed on both the cell and colloid boundaries, one might expect that the particle is repelled from the cell walls even without the presence of a NI interface. To check this, we have also calculated the free energy $U_0(y)$ of a colloidal particle immersed in a pure nematic phase ($\tau = \tau_{NI}$, $\alpha = 0$, same cell size and boundary conditions as before). Our calculations (see the upper panel of Fig. 9) demonstrate that this force is by the order of magnitude smaller, i. e. the presence of the curved interface plays a dominant role.

IV. CONCLUSIONS

To summarize, our experiments demonstrate that the curved shape of the interface and the nonuniform direc-

tor distribution next to it result in a reach dynamics of colloidal particles in the interfacial region. We show that the particles can be dragged by the interface not only horizontally, across the cell, but can also be moved in the vertical direction. This effect can be used to build heterogeneous three-dimensional photonic crystals, where the impurities (or holes) shall be positioned in designed places [34].

The drag effect can also be used to design composite materials with complex morphologies. The moving interface is able to rearrange the nucleation centers of, for example, phase-separating polymer network. During polymerization, spatial distribution of these centers affects the final morphology of the network. This opens up an opportunity to create composite materials of extraordinary properties.

[1] J. L. West, A. Glushchenko, G. X. Liao, Y. Reznikov, D. Andrienko, and M. P. Allen, Phys. Rev. E **66**, 012702 (2002).
[2] R. Zehner, K. Amundson, A. Knaian, B. Zion, and M. Johnson, SID 03 Digest p. 842 (2003).
[3] M. Ogawa, T. Takahashi, S. Saito, Y. Toko, Y. Iwakura, K. Kobayashi, and T. Akahane, SID 03 Digest p. 584 (2003).
[4] H. A. Pohl, J. Appl. Phys **22**, 869 (1951).
[5] H. A. Pohl, *Dielectrophoresis* (Cabridge University Press, Cambridge, 1978).
[6] G. H. Markx, P. A. Dyda, and R. Pethig, J. Biotechnol. **51**, 175 (1996).
[7] M. Washizu and O. Kurosawa, IEEE Trans. Ind. Appl. **26**, 1165 (1990).
[8] M. Washizu, J. Electrost. **25**, 109 (1990).
[9] H. Morgan, M. P. Hughes, and N. G. Green, Biophys. J. **77**, 516 (1999).
[10] K. Yoshinaga, M. Chiyoda, A. Yoneda, H. Nishida, and M. Komatsu, Colloid Polym. Sci. **277**, 479 (1999).
[11] P. A. Kralchevsky, N. D. Denkov, V. N. Paunov, O. D. Velev, I. B. Ivanov, H. Yoshimura, and K. Nagayama, J. Phys.-Condes. Matter **6**, A395 (1994).
[12] P. Oswald, J. Bechhoefer, and A. Libchaber, Phys. Rev. Lett. **58**, 2318 (1987).
[13] J. Ignes-Mullol, J. Baudry, L. Lejcek, and P. Oswald, Physical Review E **59**, 568 (1999).
[14] L. Blinov and V. Chigrinov, *Electrooptic Effects in Liquid Crystal Materials* (Springer-Verlag, New York, 1994).
[15] Y. A. Reznikov, V. Y. Reshetnyak, and O. V. Yaroshchuk, Zhurnal Eksperimentalnoi Teor. Fiz. **101**, 1529 (1992).
[16] B. Wen, J. H. Kim, H. Yokoyama, and C. Rosenblatt, Phys. Rev. E **66**, 041502 (2002).
[17] J. Bechhoefer, A. J. Simon, A. Libchaber, and P. Oswald, Phys. Rev. A **40**, 2042 (1989).
[18] S. Faetti and V. Palleschi, Phys. Rev. A **30**, 3241 (1984).
[19] O. D. Lavrentovich, Phys. Rev. A **46**, R722 (1992).
[20] I. M. Kulič, D. Andrienko, and M. Deserno, Europhys. Lett. **67**, 418 (2004).
[21] H. Stark, Eur. Phys. J. B **10**, 311 (1999).
[22] A. Rudinger and H. Stark, Liq. Cryst. **26**, 753 (1999).
[23] D. Voloschenko, O. P. Pishnyak, S. V. Shiyanovskii, and O. D. Lavrentovich, Phys. Rev. E **65**, 060701 (2002).
[24] P. Poulin and D. A. Weitz, Phys. Rev. E **57**, 626 (1998).
[25] P. G. de Gennes and J. Prost, *The Physics of Liquid Crystals* (Clarendon Press, Oxford, 1995), 2nd ed.
[26] M. Stephen and J. Straley, Rev. Mod. Phys. **46**, 617 (1974).
[27] M. Tasinkevych, N. M. Silvestre, P. Patrício, and M. M. Telo da Gama, Eur. Phys. J. E **9**, 341 (2002).
[28] P. Patrício, M. Tasinkevych, and M. M. Telo da Gama, Eur. Phys. J. E **7**, 117 (2002).
[29] D. Andrienko, M. Tasinkevych, P. Patricio, and M. M. T. da Gama, Phys. Rev. E **69**, 021706 (2004).
[30] N. M. Silvestre, P. Patrício, M. Tasinkevych, D. Andrienko, and M. M. Telo da Gama, J. Phys.: Condens. Matter **16**, S1921 (2004).

[31] D. Andrienko, M. Tasinkevych, and S. Dietrich, Europhys. Lett. **70**, 95 (2005).

[32] H. J. Coles, Mol. Cryst. Liq. Cryst. **49**, 67 (1978).

[33] S. Kralj, S. Žumer, and D. W. Allender, Phys. Rev. A **43**, 2943 (1991).

[34] J. L. West, A. Glushchenko, G. X. Liao, Y. Reznikov, D. Andrienko, and M. P. Allen, Mol. Cryst. Liq. Cryst. **410**, 611 (2004).